Journal of
SHIP RESEARCH

Water Tunnel Tests of Three Vented Hydrofoils in Two-Dimensional Flow

By Thomas G. Lang[1] and Dorothy A. Daybell[1]

This paper provides information, based primarily on experimental results, for use in the design of vented hydrofoils. Data are presented on hydrofoils that are vented to provide a control force as an alternative to the use of flaps. Also included are data on lifting hydrofoils that are vented to reduce their susceptibility to cavitation and to provide improved lift-to-drag ratios at high speeds.

DURING a search at the Naval Ordnance Test Station (NOTS) for improved methods of torpedo control, it was proposed[2] that the pressure be changed on a portion of a shroud-ring stabilizer by exhausting gas through a hole in the surface of the ring. This idea was related to previous speculation on lifting hydrofoils which would be continuously vented to provide improved high-speed performance. As a result of these ideas, an experimental study[3] was conducted in the High Speed Water Tunnel at the California Institute of Technology (CIT). Three two-dimensional hydrofoil models were tested with air exhausted through their surfaces at various chordwise locations. Two of the models were streamlined in cross section and were vented through a spanwise port in the upper surface; the third model had a blunt trailing edge (or base) and was vented only at the base.

The objects of the tests were to determine (*a*) how the lift, drag, and moment were affected by exhaust point, cavity pressure, and hydrofoil shape; (*b*) whether the air would move forward of the exhaust point; and (*c*) how the cavity pressure varied with air-flow rate.

The results indicate that when sufficient air or gas is exhausted through the surface of a hydrofoil, the cavity collapses behind the hydrofoil and the forces are markedly changed but are steady. For example, exhausting air through the upper surface of a streamlined hydrofoil reduces the lift coefficient as much as 0.6 at zero angle of attack. This reduction in lift coefficient becomes greater as the angle of attack is increased. The lift-coefficient derivative varied linearly from 2π with the per cent exhaust point at the trailing edge to π with exhaust from the 3 per cent chord point.

The air was not observed to move forward of the exhaust point unless boundary-layer separation or excessive vapor cavitation occurred ahead of this point. As the air flow to each hydrofoil increased it passed a critical value, $Q_{cr}' = 0.07$, beyond which the cavity pressure and the forces on the hydrofoil were steady and essentially constant. This condition was called "fully vented." Hysteresis was found at certain angles of attack wherein the hydrofoil remained fully vented as the air-flow rate reduced again below the critical air-flow rate.

The drag of the blunt-based hydrofoil was considerably reduced by base ventilation. The lift, lift-curve slope, and moment remained essentially unchanged from the fully wetted condition and were found to be about the same as those of a streamlined hydrofoil having the same camber line.

The measured lift-to-drag ratios of the various vented hydrofoils were lower than those of conventional streamlined fully wetted hydrofoils, but lay in the same range.

Vapor cavitation tests indicated that base-vented hydrofoils may be more useful in providing lift at high speeds than conventional streamlined hydrofoils.

Test Outline

The profiles of the three models are shown in Fig. 1. Fig. 2 is a drawing of hydrofoil A, showing the model dimensions, one of the exhaust ports, several pressure taps, and the tubing that passed through the tunnel wall. Hydrofoil A had an NACA 0010 thickness distribution and a design lift coefficient of 0.2 with the NACA "$a = 1.0$" (uniform load) mean line. Hydrofoil B had an uncambered NACA 65_2-015 cross section, modified by replacing the cusp-shaped rear section with a wedge tangent at the 60 per cent chord point. Hydrofoil C had a parabolic thickness distribution with a blunt trailing edge, a thickness-to-chord ratio t/c of 0.15, and a design lift co-

[1] U. S. Naval Ordnance Test Station, Pasadena, Calif.
[2] By Kenneth E. Smith of NOTS.
[3] Conducted from June 1958 to June 1959 under Bureau of Ordnance funding.

efficient of 0.4 with the NACA "$a = 1.0$" mean line.

With Hydrofoils A and B, the air was exhausted through a spanwise row of 55 holes (0.012 in. diam) in the upper surface. The chordwise location, a, of the exhaust point on Hydrofoil A was varied for different runs and was located at a/c values of 0.031, 0.188, 0.300, 0.312, 0.641, and 0.828, where c is the chord length. The exhaust point on Hydrofoil B was located at $a/c = 0.30$. Air was exhausted through a single hole in the base of Hydrofoil C.

The models had a span b of 2.9 in. and a chord c of 4.0 in. They were tested in a two-dimensional working section 14 in. high in the CIT High Speed Water Tunnel [1].[4]

The cavity pressure, lift, drag, and moment were measured on all hydrofoils as a function of angle of attack, air-flow rate, and tunnel velocity and pressure. In addition, the chordwise pressure distribution was measured on Hydrofoil A when fully wetted and when vented with $a/c = 0.30$. The incipient vapor cavitation number was obtained at the leading edge of Hydrofoil C as a function of angle of attack. The majority of the tests were conducted at a free-stream velocity V_∞ of 30 fps and a free-stream static pressure P_∞ of 2280 psf.

A more detailed description of the experimental procedures, additional detailed data and analysis, and more photographs of the experiments are included in two reports published by the Naval Ordnance Test Station [2, 3].

The data reported in this paper have been corrected only for the frictional drag of the wall-support disk on which the models were mounted. Further corrections for most of the tunnel interference effects have been evaluated in [2] and [3]. In general, these corrections were found to be small.

[4] Numbers in brackets designate References at the end of the paper.

Results

Nature of the Flow

Under most conditions the air did not move forward of the exhaust point. A low air-flow rate produced a small local cavity from which air bubbles streamed rearward. With Hydrofoils A and B, an increase in air-flow rate produced a longer cavity on the hydrofoil surface, causing the forces to become increasingly unsteady until the end of the cavity approached the trailing edge. At this point, a slight increase in air-flow rate caused the cavity to suddenly spring free of the hydrofoil and terminate at a point about two chord lengths downstream. In this fully vented condition the forces were steady but quite different from the fully wetted forces. With Hydrofoil C, the air tended to collect in pockets in the vortices behind the base until the flow rate was increased to a critical value beyond which the vortices disappeared and a long air-filled cavity formed behind the base. This condition was also called fully vented. The minimum air-flow rate required to produce the fully vented condition was called the "critical" air-flow rate. Photographs of the fully vented and partially vented flows are shown in Fig. 3.

In all the tests, the air did not spring forward to the leading edge unless the angle of attack approached the

Nomenclature

The foot-pound-second-radian system of units is used, unless otherwise stated.

a = chordwise distance from leading edge to exhaust point
b = span of hydrofoil
c = chord of hydrofoil
C_D = drag coefficient $\left(\frac{\text{drag}}{bc\,q_\infty}\right)$
C_{D_f} = frictional drag coefficient
C_L = lift coefficient $\left(\frac{\text{lift}}{bc\,q_\infty}\right)$
C_{L_0} = lift coefficient at $\alpha = 0°$
C_{L_α} = lift-coefficient derivative $\left(\frac{dC_L}{d\alpha}\right)$
C_M = moment coefficient about quarter-chord point $\left(\frac{\text{pitching moment}}{bc^2\,q_\infty}\right)$
C_P = local pressure coefficient $\left(\frac{P-P_\infty}{q_\infty}\right)$
C_Q = air-flow-rate coefficient based on planform area $\left(\frac{Q}{bc\,V_\infty}\right)$
$C_{Q_{cr}}$ = value of C_Q at which hydrofoil first becomes fully vented
D' = drag coefficient based on base area $\left(\frac{\text{drag}}{bt\,q_\infty}\right)$
K = ventilation number $\left(\frac{P_\infty - P_c}{q_\infty}\right)$
L/D = lift-to-drag ratio
P = local static pressure on surface of hydrofoil
P_c = base or cavity pressure
P_∞ = free-stream static pressure
q_∞ = free-stream dynamic pressure ($\frac{1}{2}\rho V_\infty^2$)
Q = air flow rate
Q' = alternate air-flow-rate coefficient based on streamwise projection of air-covered surface of hydrofoil $\left(\frac{Q}{bt\,V_\infty}\right)$
Q_{cr}' = value of Q' at which hydrofoil first becomes fully vented
t = base thickness or streamwise projection of air-covered surface of hydrofoil
V_∞ = free-stream velocity
x = chordwise distance from leading edge
y = perpendicular distance from x-axis of hydrofoil to point on hydrofoil surface
α = angle of attack
ρ = density of water
σ = free-stream (vapor) cavitation number $\left(\frac{P_\infty - P_v}{q_\infty}\right)$
σ_i = incipient (vapor) cavitation number

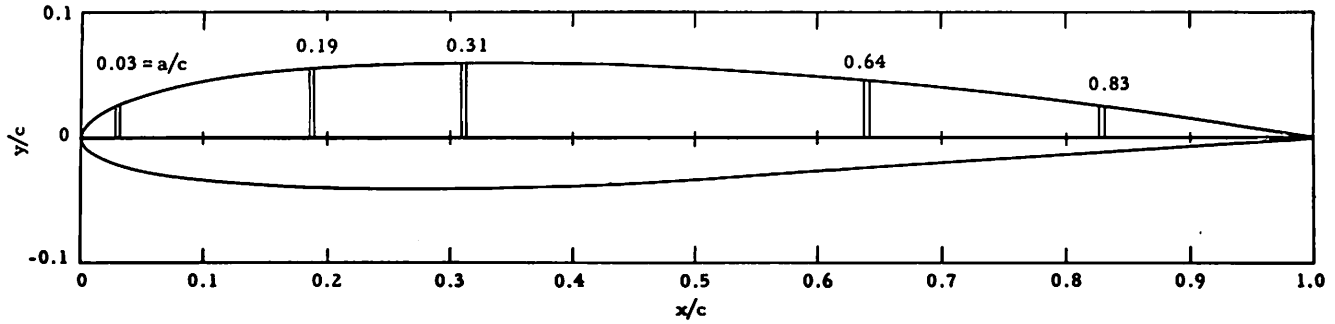

(*a*) Hydrofoil A

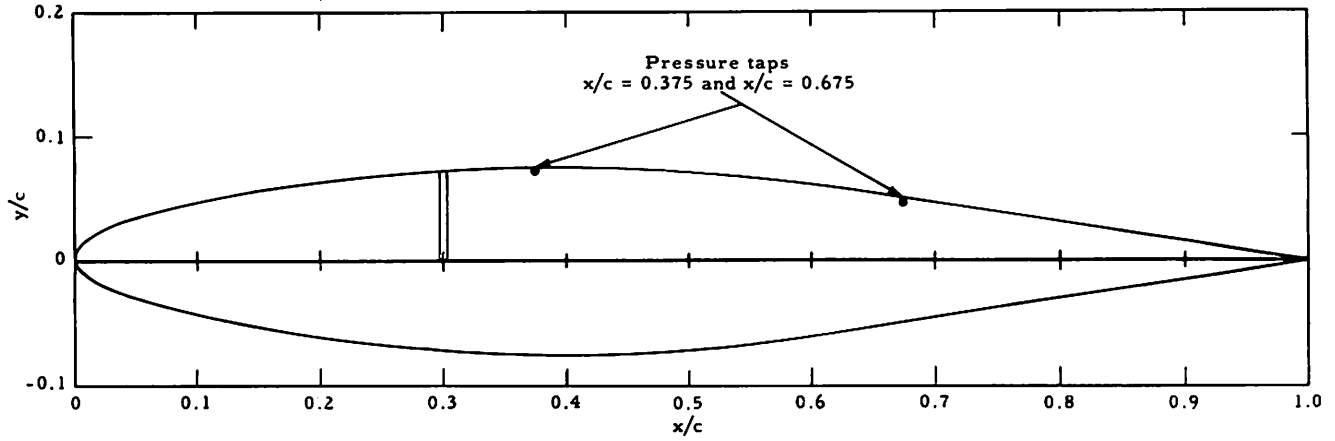

(*b*) Hydrofoil B

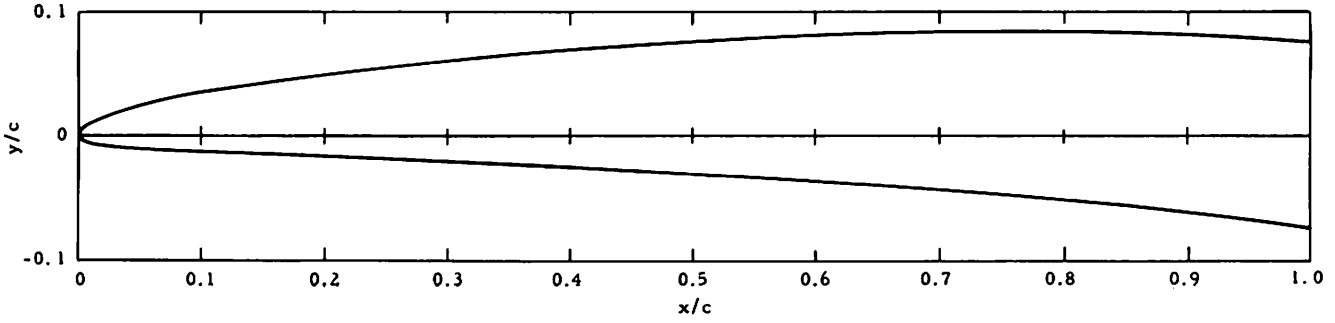

(*c*) Hydrofoil C

Fig. 1 Profiles of the three hydrofoil models

normal stall angle of the hydrofoil, or unless a patch of vapor cavitation was produced at the leading edge that extended rearward into the air cavity. Pressure surveys showed that the static pressure on the wetted surface ahead of an air cavity could be much lower than cavity pressure without the air cavity springing forward. With Hydrofoil C, at certain values of angle of attack and cavity pressure, the cavity intermittently moved forward of the exhaust point in the form of a thin layer that extended about $^1/_4$ in. ahead of the base. It is believed that the boundary layer had separated and that the air was drawn from the cavity into this region. Only a small effect on lift was observed as a result of this type of local ventilation. Modification of the hydrofoil surface ahead of the base would probably prevent this type of ventilation, since it was not observed in the two-dimensional tests of Hydrofoils A and B.

Cavity Pressure and Air-Flow Rate

It was difficult to measure the cavity pressure until the hydrofoils were fully vented because of the fluctuating pattern of the flow at low air-flow rates. In general, the

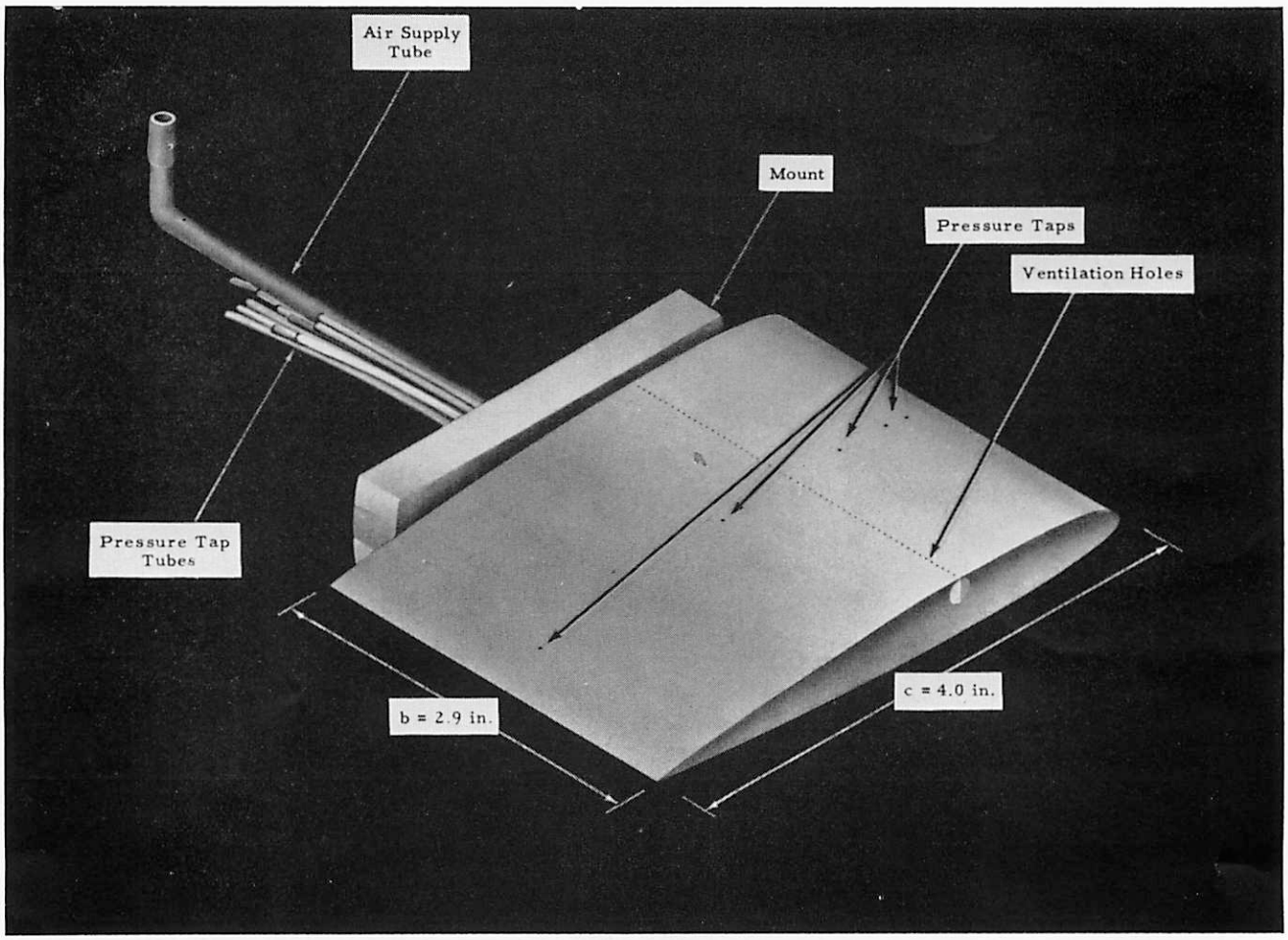

Fig. 2 Detailed view of Hydrofoil A

cavity pressure increased rapidly with increasing air-flow rate until the hydrofoil was fully vented. The cavity pressure then remained nearly constant no matter how much the air-flow rate was increased. During the analysis of the data, a unique relationship was found for the critical air-flow rate if an alternate air-flow-rate coefficient Q' was used instead of the standard C_Q. Q' is based upon the reference area bt, where t is defined as the thickness of the projection, in the rearward free-stream direction, of the air-covered portion of the hydrofoil surface. The sketch in Fig. 5 illustrates how t is obtained. (It should be noted that t varies with angle of attack and ventilation point, and that t is not defined for those attitudes where the hydrofoil surface interferes with the projection.) The critical air-flow-rate coefficient for fully vented flow, Q_{cr}', was found to be essentially a constant for the three hydrofoils, independent of hydrofoil contour, angle of attack, and ventilation point. This value of Q_{cr}' was 0.07. Fig. 4 shows the ventilation number K versus Q' for the three hydrofoils at $\alpha = 0°$. (The data for other angles of attack near zero were similar.) The values of K plotted for no air-flow rate were set equal to $-C_P$ in fully wetted flow, where C_P is the pressure coefficient.

A hysteresis effect was found at certain angles of attack, wherein the hydrofoil remained fully vented as the air-flow rate was reduced from a high value to values somewhat below the critical rate. The airflow rate and hysteresis are undoubtedly affected by tunnel wall interference, free-stream water turbulence, model roughness, Reynolds number and model contour. It is definitely known that the cavity pressure was affected by the tunnel-wall interference, since it did not approach a value near free-stream pressure with increasing air-flow rate, as it otherwise should have. A new series of tests is currently being conducted in the Free Surface Water Tunnel at CIT to investigate more fully air-flow rates, cavity pressures, and hydrofoil drag.

Lift

The lift coefficient C_L was reduced by as much as 0.4 on Hydrofoil A and 0.5 on Hydrofoil B at $\alpha = 0°$ when they were fully vented by exhausting air through their upper surfaces, as shown in Figs. 5 and 6. The tests on Hydro-

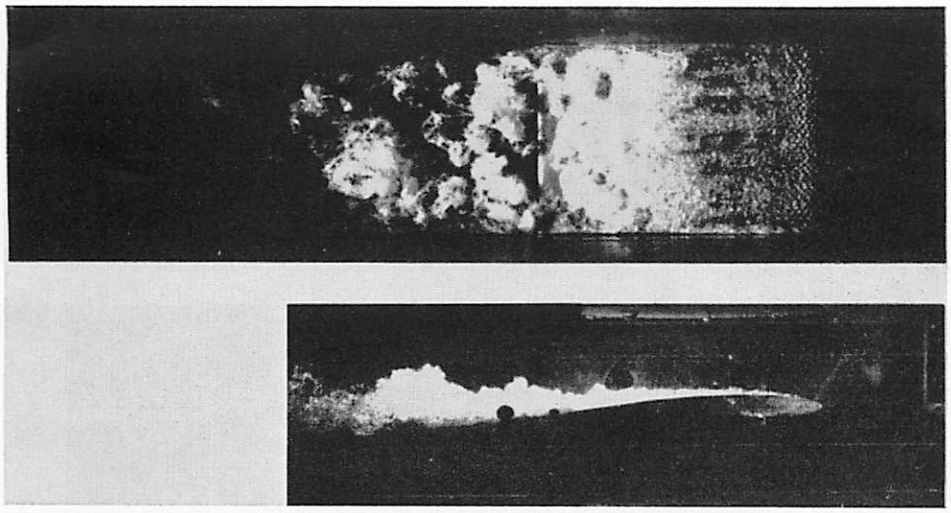

(*a*) Hydrofoil A, $a/c = 0.03$, partially vented

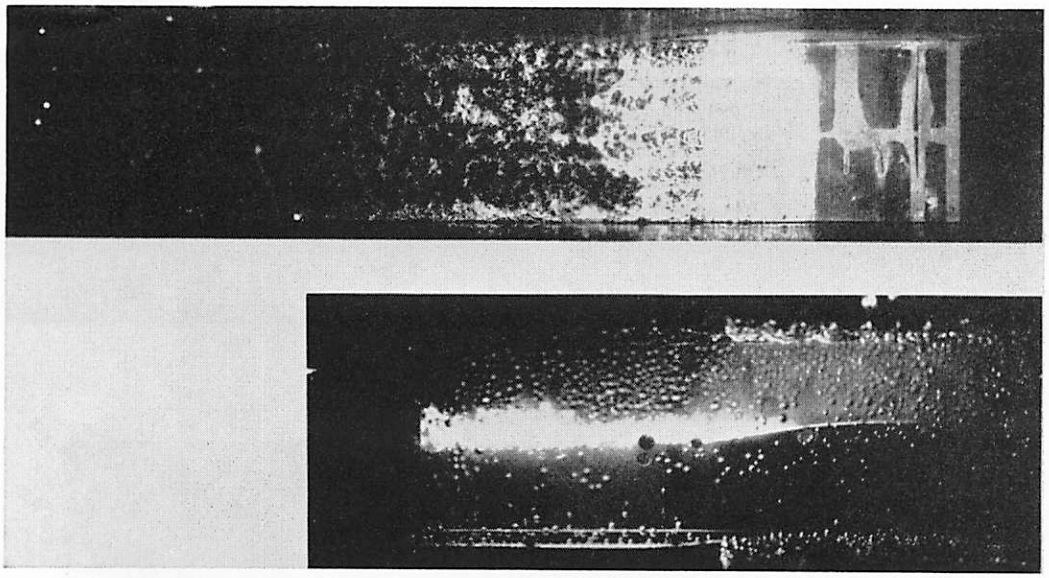

(*b*) Hydrofoil A, $a/c = 0.64$, fully vented

Fig. 3 Top and side views of fully vented and partially vented flow

foil A with various exhaust points showed that the lift reduced further from the fully wetted value as the exhaust point approached the leading edge and as the angle of attack increased.

The tests on all models showed that the lift coefficient derivative, C_{L_α}, varied linearly from about 2π with the exhaust point at the trailing edge to π with exhaust at $a/c = 0.03$. The data are in excellent agreement, for $a/c \geq 0.25$, with equation (1) based on linearized theory for $K = 0$ as in [4]:

$$C_{L_\alpha} = 2\pi \left[\frac{1 + (a/c)^{1/2}}{2} \right]^2 \qquad (1)$$

The deviation from theory when $a/c < 0.25$ is believed to have been caused by the interference of the underlying hydrofoil surface with the cavity, and by tunnel-wall interference.

The lift of Hydrofoil C remained essentially the same whether it was wetted or vented, as shown in Fig. 7. Included in Fig. 7 are data [5] for a streamlined airfoil with the same camber as Hydrofoil C. The lift coefficient and lift-coefficient derivative of the base-vented hydrofoil are essentially the same as those of the streamlined airfoil. Since the camber was arbitrarily selected, it was believed that this result is general in the sense that any plot of C_L versus α is independent of thickness distribu-

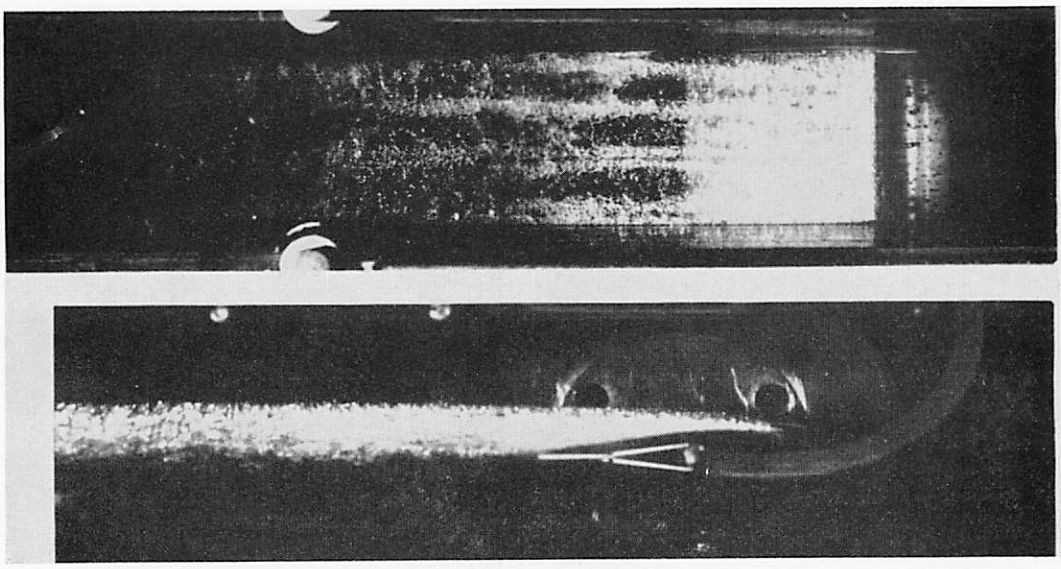

(*c*) Hydrofoil B, $a/c = 0.30$, fully vented

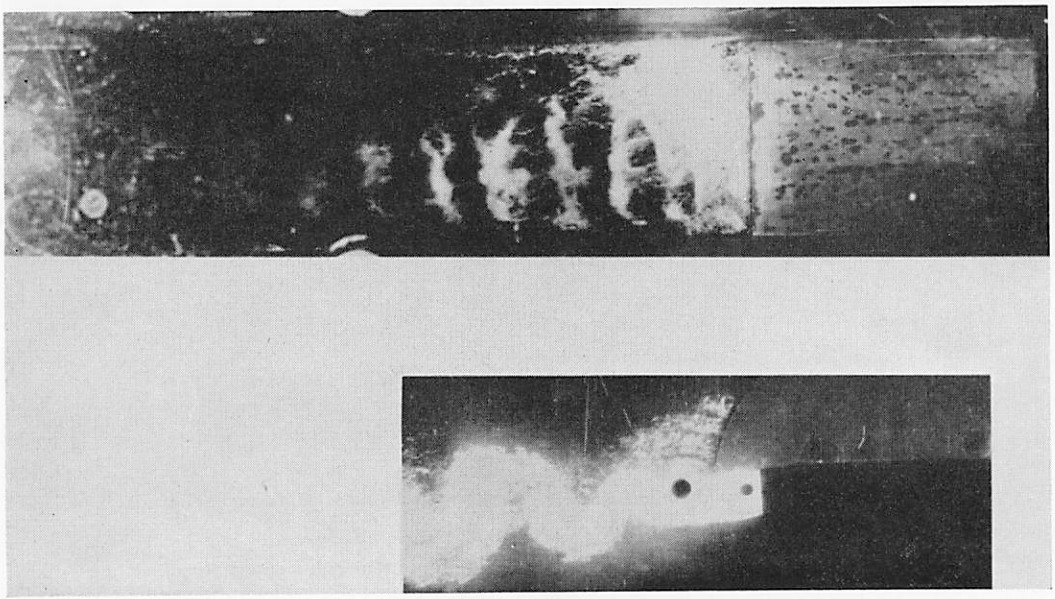

(*d*) Hydrofoil C, $a/c = 1.00$, partially vented

Fig. 3 (*Continued*)

tion and trailing-edge venting and is dependent only on camber. Subsequent to these experiments, it was shown [6] to be general in theory as long as no separated flow or ventilation occurs ahead of the trailing edge. It is therefore expected, for example, that if the rear portion of the lower surface of a base-vented hydrofoil were deflected as a split flap, the resulting lift force would be the same as that produced by the resulting camber or, in other words, half that produced by deflecting both the upper and lower surfaces as a plain flap.

Curves of C_L versus C_Q for Hydrofoil A with $a/c = 0.30$ are shown in Fig. 8. The previously mentioned hysteresis effect is seen in the data for $\alpha = 1.6°$.

Drag

The drag of the streamlined Hydrofoils A and B increased rapidly as the air-flow rate was increased toward the critical value. Once the hydrofoils were fully vented, their drag suddenly reduced to a steady value that was still somewhat higher than the fully wetted drag. The drag of the blunt-based Hydrofoil C however, reduced rapidly as the air-flow rate was increased, and ap-

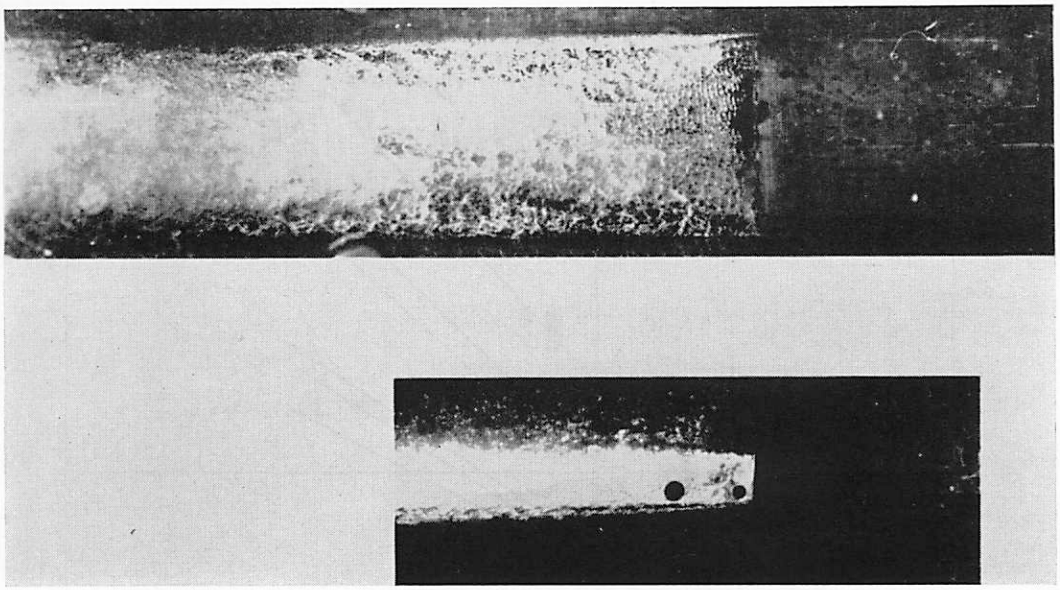

(*e*) Hydrofoil C, $a/c = 1.00$, fully vented

Fig. 3 (*Continued*)

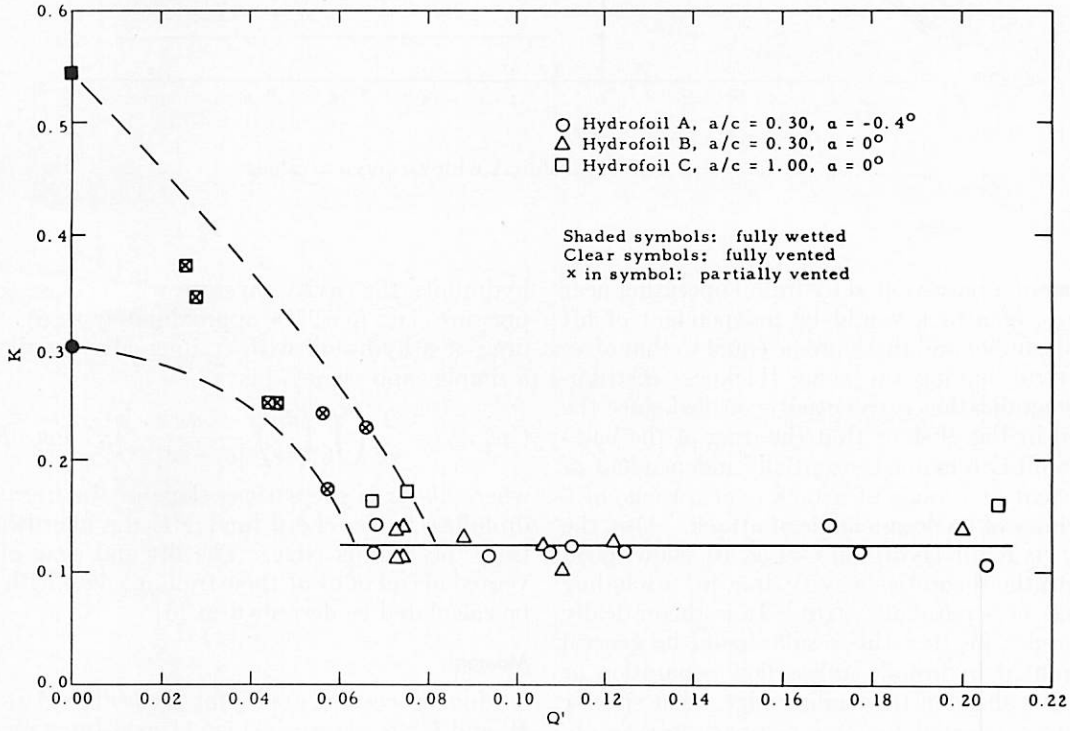

Fig. 4 K versus Q' for the three hydrofoils at $\alpha \cong 0°$.

proached a minimum value when the hydrofoil became fully vented. This minimum value was still higher than the fully wetted frictional drag of a streamlined hydrofoil. Fig. 9 shows the drag coefficient C_D versus α for Hydrofoils A (with $a/c = 0.30$), B, and C in fully wetted and fully vented flow. In all cases of fully vented flow, the drag would have been lower if the cavity pressure had more closely approached the free-stream pressure, as it would have done without tunnel-wall blockage.

One objective of this test program was to determine if

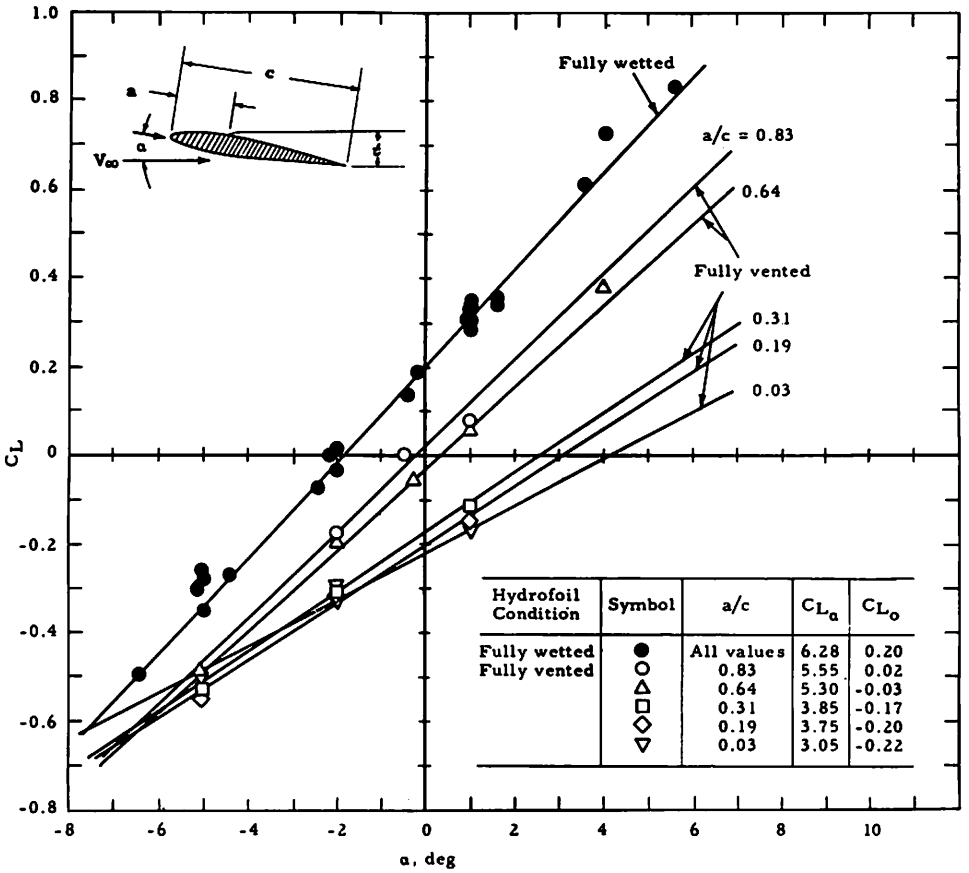

Fig. 5 C_L versus α for Hydrofoil A with various a/c values

the cavity drag of a base-vented hydrofoil operating near its design angle of attack would be independent of lift coefficient and camber and therefore be equal to that of an uncambered strut having the same thickness distribution. This generalization is essentially verified since the results plotted in Fig. 9 show that the drag of the base-vented Hydrofoil C remained essentially independent of the lift coefficient and angle of attack over a range of 6 deg in the vicinity of its design angle of attack. Also, the plot of D' versus K for Hydrofoil C, Fig. 10, shows good agreement with the theoretical cavity drag [6] (excluding frictional drag) of a parabolic strut. It is theoretically shown in reference [6] that this result should be general for all base-vented hydrofoils unless flow separation or ventilation exists ahead of the trailing edge. The specific theoretical curve selected for this comparison was obtained from linearized cavity-flow theory using an "open-cavity" model wherein the cavity terminates at its widest point and is followed by a wake (or cavity) of constant thickness similar to that observed in these experiments. This theoretical result is shown [6] to be similar to but slightly different from that obtained using the linearized theory of [7] or [8] for a "closed-cavity" model.

In most instances of practical application of vented hydrofoils, the cavity pressure will be close to the depth pressure (i.e., K will be approximately zero). The cavity drag of a hydrofoil with trailing-edge ventilation, using a simple expression [7] is

$$C_{D\,\text{cavity}} = \frac{2}{\pi c}\left(\int_0^c \left(\frac{dy}{dx}\right)\frac{dx}{[c-x]^{1/2}}\right)^2, \quad \text{for} \quad K = 0 \quad (2)$$

where dy/dx is the surface slope of the uncambered hydrofoil, c is the chord, and x is the chordwise distance from the leading edge. The lift and drag of hydrofoils vented ahead of or at their trailing edges with $K \geqq 0$ can be calculated as described in [6].

Moment

Moment coefficients C_M for Hydrofoils A ($a/c = 0.30$), B, and C are shown in Fig. 11 as a function of angle of attack. The moment coefficient of Hydrofoil C remained essentially unaffected by ventilation. The moment coefficients of Hydrofoils A and B, however, were considerably increased by ventilation, thereby indicating a forward movement of the center of pressure.

Ventilation Efficiency

When a hydrofoil is vented for control purposes, the efficiency of the ventilation may be defined as the change

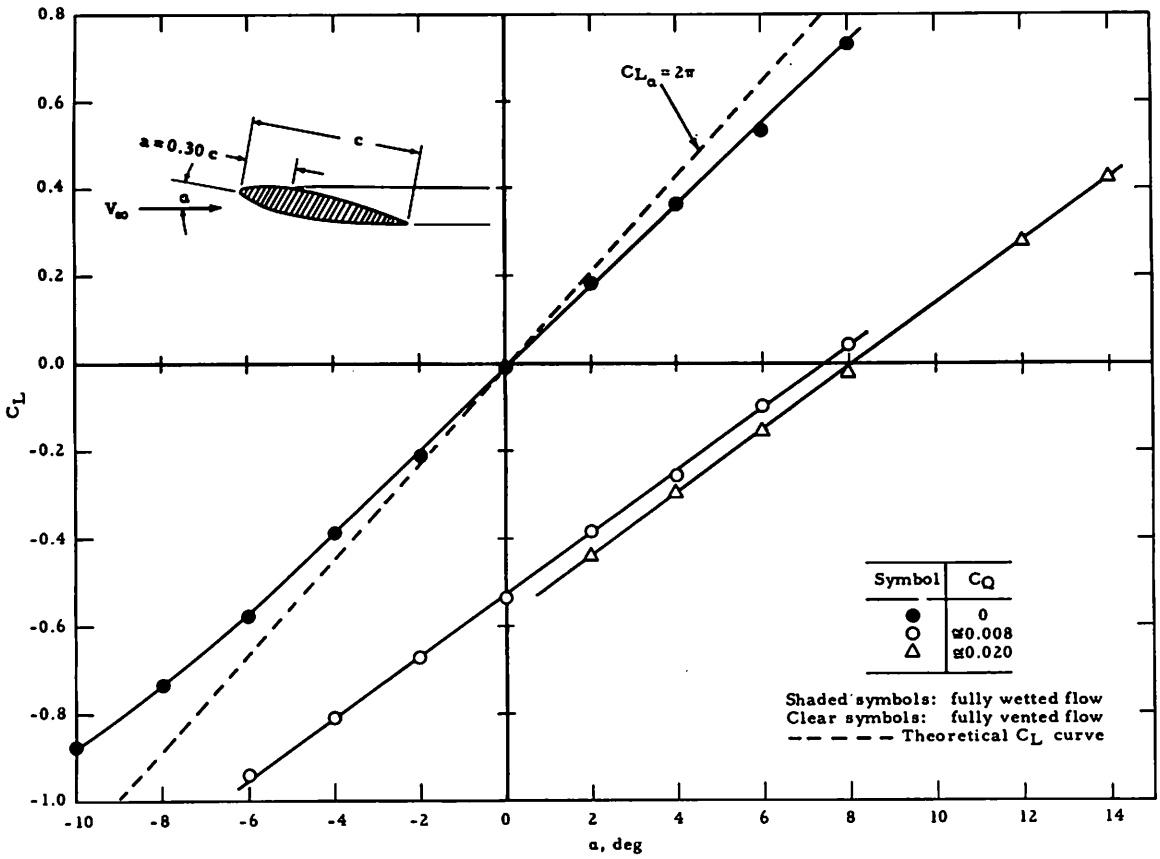

Fig. 6 C_L versus α for Hydrofoil B with $a/c = 0.30$

in lift per unit gas flow rate:

$$\frac{\Delta C_L}{C_{Q\,cr}} = \frac{(C_L \text{ at } C_Q = 0) - (C_L \text{ at } C_Q = C_{Q\,cr})}{C_{Q\,cr}} \quad (3)$$

Ventilation efficiencies for Hydrofoils A and B are shown in Fig. 12 as a function of angle of attack. The ventilation efficiency of Hydrofoil A was a maximum near zero angle of attack and for exhaust points between $a/c = 0.20$ and $a/c = 0.70$. The change in lift, as stated previously, was greatest when the exhaust point approached the leading edge. Consequently, a maximum control force is obtained most efficiently when gas is exhausted in the region of the 20 and 30 per cent chord points. Proportional control could be obtained by exhausting gas at various points to fully vent the hydrofoil. Varying the gas-flow rate at a given point for proportional control would be less desirable because the forces are unsteady in the range where the control force is variable.

Lift-to-Drag Ratio

Hydrofoils A and B were designed to operate fully wetted most of the time and fully vented when control is desired. Hydrofoil C was designed to operate fully vented all of the time and to provide good L/D ratios. To obtain more information on the lift-to-drag ratio L/D of continuously vented hydrofoils, the data for Hydrofoils A (with $a/c = 0.30$) and B were re-interpreted, assuming that they would operate continuously vented. These hydrofoils would have higher values of L/D if they were inverted so that their cavities were on their lower surfaces. Therefore, the portion of L/D data plotted in Fig. 13 for the fully vented Hydrofoils A and B pertains to lower surface ventilation. It is seen in Fig. 13 that L/D values of the Hydrofoils A, B, and C were 43.0, 28.8, and 11.0, respectively, when fully wetted, and 29.4, 33.5, and 21.6, respectively, when fully vented. The L/D ratios of the fully vented hydrofoils are therefore comparable to those of the fully wetted hydrofoils. Higher L/D ratios would have been obtained for the vented hydrofoils if K had approached zero and if the effective camber of the fully vented hydrofoils had been greater. By "greater effective camber" is meant an increase in the convexity of the upper wetted surface and a decrease in the convexity of the lower wetted surface.

The theoretical L/D ratios and incipient cavitation numbers of a variety of vented hydrofoils are presented and analyzed in reference [9]. Fig. 14 shows some of the results for several two-dimensional fully vented and fully wetted hydrofoils. It was assumed that the boundary layer was turbulent, K was zero, that each hydrofoil was noncavitating, and that each had the same

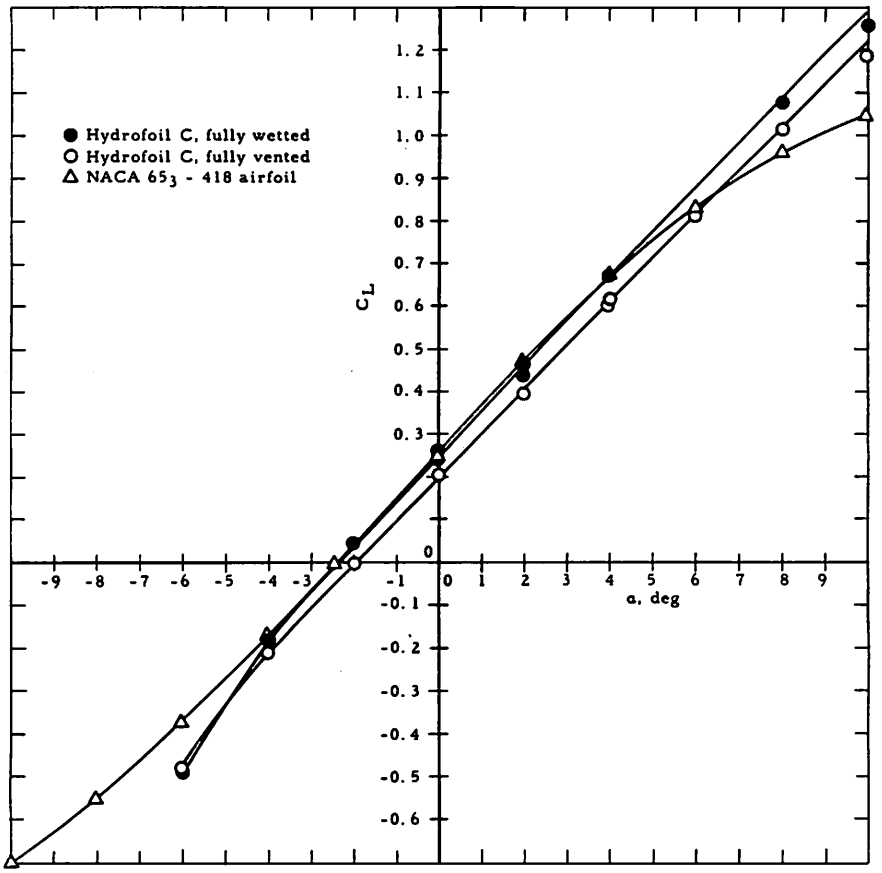

Fig. 7 C_L versus α for Hydrofoil C and for NACA 65_3-418 airfoil

lift and bending strength as an NACA 16-510 hydrofoil. It is seen that, for a given cavitation number σ, a type of vented hydrofoil exists that is theoretically more efficient than a well-designed streamlined hydrofoil. The drag of a vented hydrofoil can be minimized by designing its pressure distribution to maximize the extent of laminar flow.

Pressure Distribution

As one would expect, the static pressure distribution on both sides of Hydrofoil A was markedly affected when air was exhausted through the upper surface. When the hydrofoil was fully vented, the static pressure on the air-covered surface and at each edge of the cavity was equal to the cavity pressure. Fig. 15 shows typical static pressure distributions on the upper and lower surfaces of the hydrofoil when it was fully wetted and fully vented with $a/c = 0.30$.

Cavitation Inception

The measured incipient (vapor) cavitation number σ_i for Hydrofoil C is shown versus α in Fig. 16, together with a theoretical curve derived using references [5], [10] and [11]. The differences between experiment and theory may be attributed to the effects of dissolved air in the tunnel water, to deviations of the leading-edge radius from the design radius, to tunnel-wall interference, and to the reduction in the design lift coefficient which is typical of the NACA "$a = 1.0$" mean line.

At zero angle of attack, both theory and experiment showed σ_i to be significantly lower than that of a streamlined hydrofoil having the same camber and maximum thickness. In theory, the cavitation resistance of a hydrofoil reduces (σ_i increases) approximately as the square of the angle of attack and as the reciprocal of the design leading-edge radius. It is noted, however, that for the same thickness-to-chord ratio, the parabolic hydrofoil has a leading-edge radius equal to about half that of a streamlined hydrofoil, and is therefore more affected by large deviations from the design angle of attack. If necessary, a parabolic hydrofoil may be designed to operate over a larger angle-of-attack range without cavitating by making its thickness-to-chord ratio larger at the expense of increased cavity drag. Fortunately, if the cavity drag is found to be excessive, it may be reduced by modifying the thickness distribution from that of a parabola to one more like an ellipse with a cut-off trailing edge such as the modified 16-510 hydrofoil shown in Fig. 14. This latter shape is slightly more susceptible

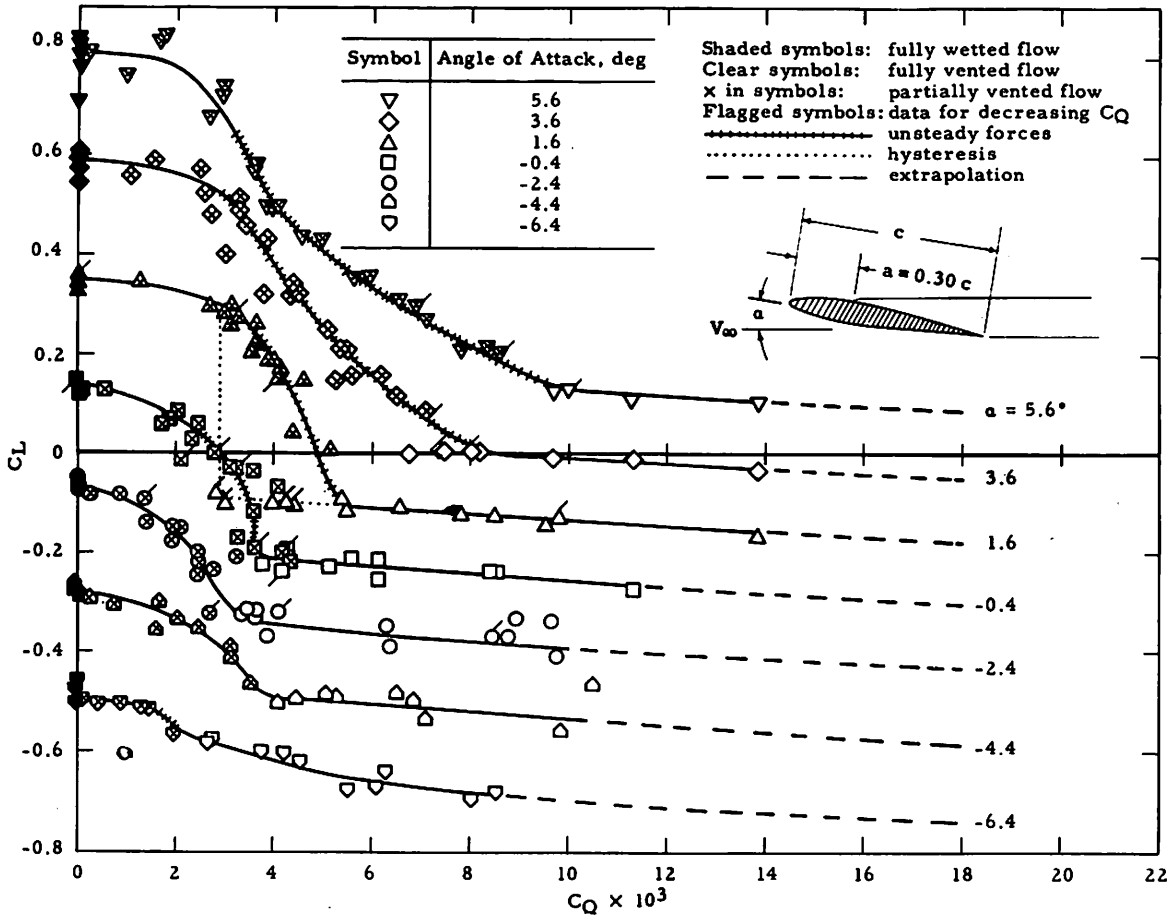

Fig. 8 C_L versus C_Q for Hydrofoil A, $a/c = 0.30$, at various angles of attack

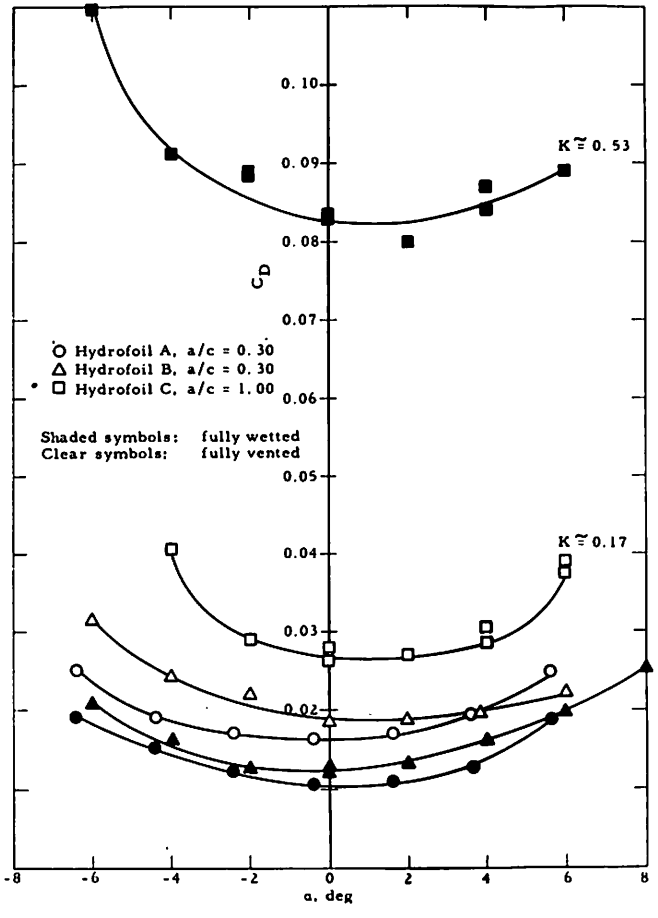

Fig. 9 C_D versus α for the three hydrofoils

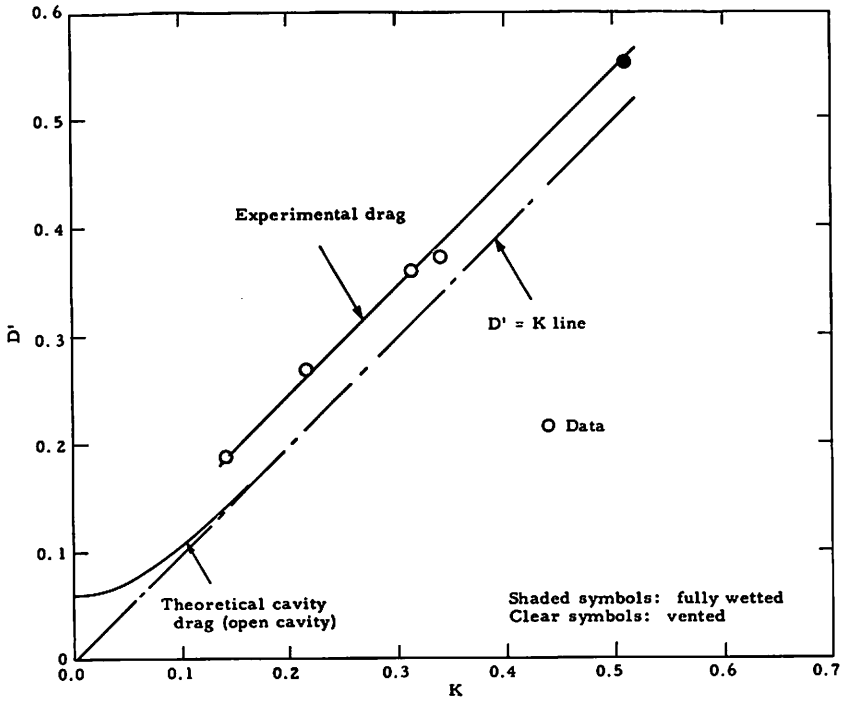

Fig. 10 D' versus K at $\alpha = 0°$, experiment and theory

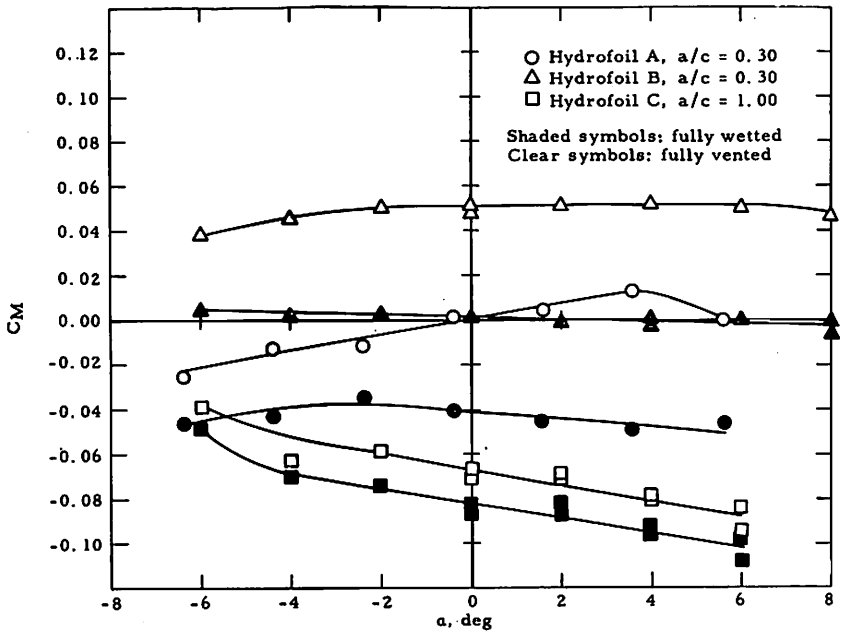

Fig. 11 C_m versus α for the three hydrofoils

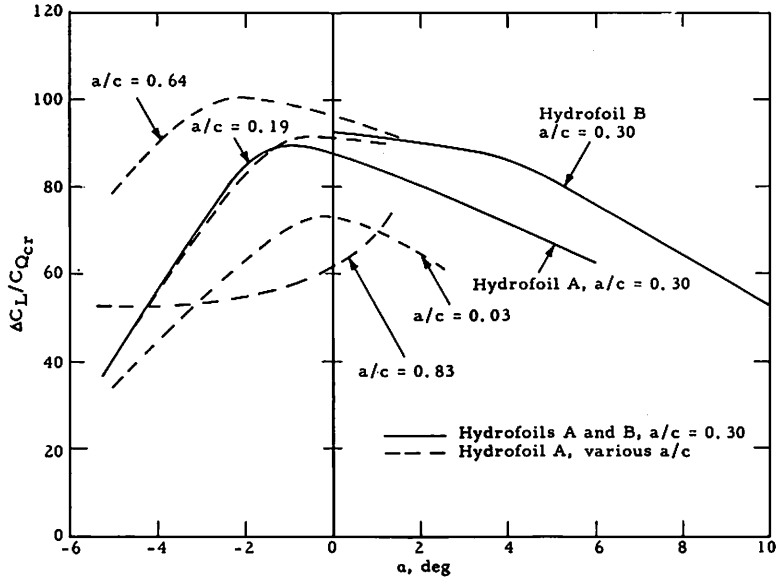

Fig. 12 Ventilation efficiency versus angle of attack for Hydrofoils A and B

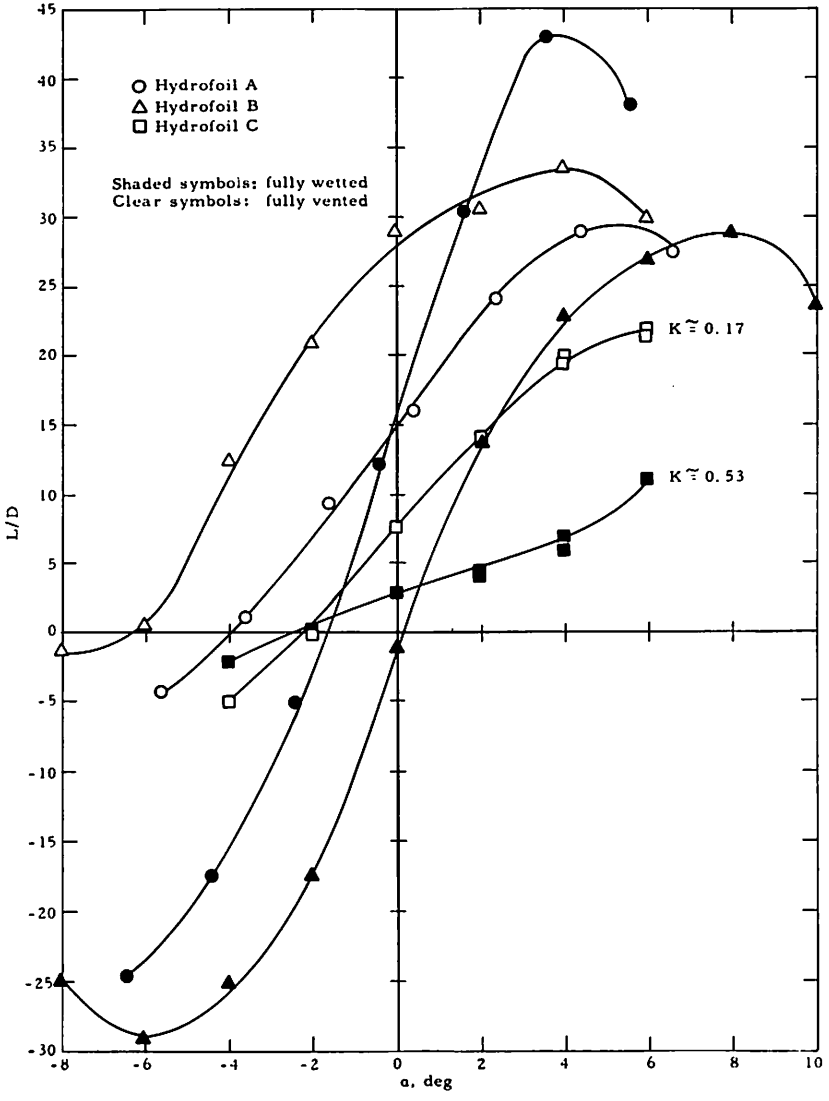

Fig. 13 L/D versus α

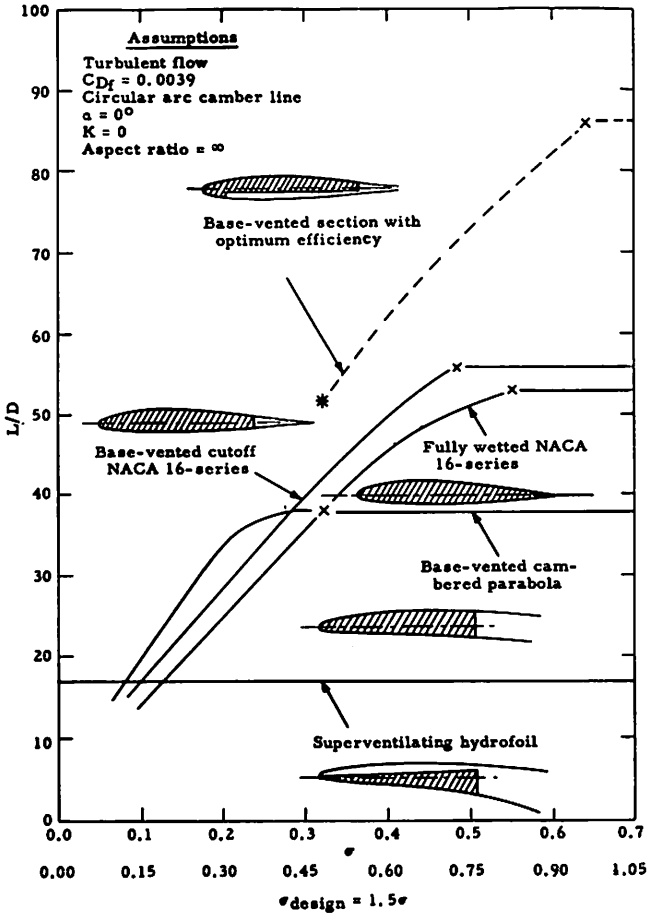

Fig. 14 Comparison of hydrofoils with strength and lift equal to those of the NACA 16-510 hydrofoil

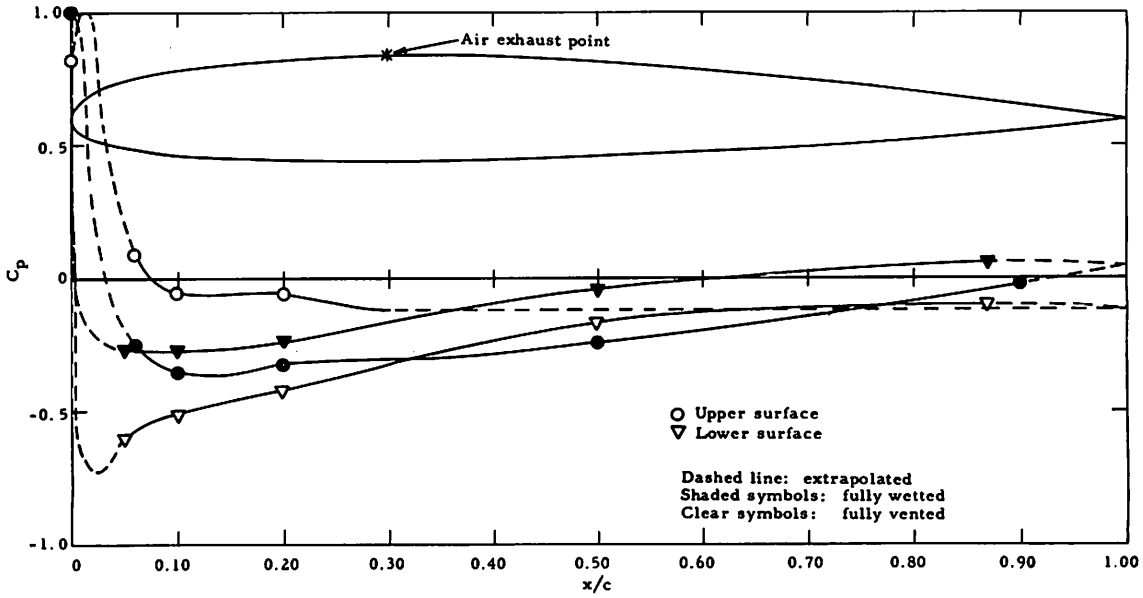

Fig. 15 C_p versus x/c for Hydrofoil A, $a/c = 0.30$, $\alpha = -0.4°$

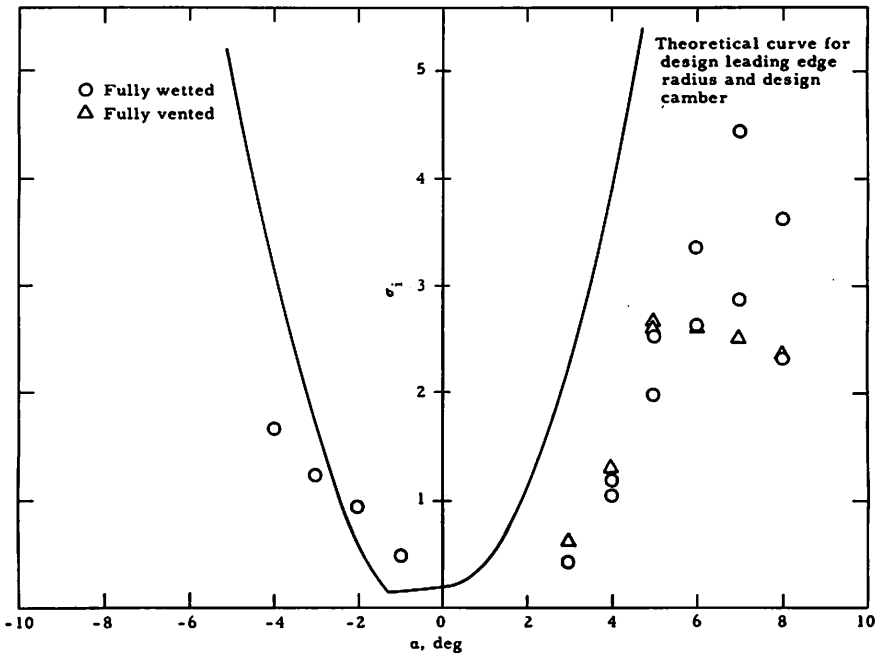

Fig. 16 σ_i versus α, experiment and theory

to cavitation at the design angle of attack than the parabola but is less susceptible to cavitation at large off-design angles because of its greater leading-edge radius.

Example of Gas-Ventilation Control

To compare gas-ventilation control with flap control, the following example is analyzed:

Consider Hydrofoil B, in two-dimensional flow, at $\alpha = 0°$, with the exhaust point at $a/c = 0.30$. From Fig. 6 it is seen that C_{L_0} is changed from 0, fully wetted, to -0.54, fully vented. The gas-flow rate required to produce this control force may be estimated from Fig. 12:

$$\frac{\Delta C_L}{C_{Q_{cr}}} = 92$$

$$\Delta C_L = +0.54$$

$$C_{Q_{cr}} = 0.0059 = \frac{Q_{cr}}{bcV_\infty}$$

The deflection of a typical 30 per cent chord trailing-edge flap on a two-dimensional hydrofoil having the same shape must be 10 deg to produce the same control force [12].

Acknowledgments

The authors appreciate the assistance of Mr. Taras Kiceniuk at the California Institute of Technology, who supervised the operations of the water tunnel and together with Profs. V. A. Vanoni, A. J. Acosta, and T. Y. Wu, contributed many valuable suggestions to the experiment.

The participation of Mr. K. E. Smith in the water-tunnel tests of Hydrofoil A is also gratefully acknowledged.

The discussions with Mr. A. G. Fabula concerning linearized cavity theory were useful in presenting that aspect of this paper.

References

1 R. T. Knapp, J. Levy, P. O'Neill, and F. B. Brown, "The Hydrodynamics Laboratory of the California Institute of Technology," *Trans. ASME*, vol. 70, 1948, pp. 437–457.

2 T. G. Lang, D. A. Daybell, and K. E. Smith, "Water-Tunnel Tests of Hydrofoils with Forced Ventilation," NAVORD Report 7008, NOTS TP 2363, November 10, 1959.

3 T. G. Lang and D. A. Daybell, "Water-Tunnel Tests of a Base-Vented Hydrofoil Having a Cambered Parabolic Cross Section," NAVWEPS Report 7584, NOTS TP 2569, October 10, 1960.

4 A. G. Fabula, "Theoretical Lift and Drag on Vented Hydrofoils for Zero Cavity Number and Steady Two-Dimensional Flow," NAVORD Report 7005, NOTS TP 2360, November 4, 1959.

5 I. H. Abbott, A. E. von Doenhoff, and L. S. Stiverd, "Summary of Airfoil Data," NACA Report 824, 1945.

6 A. G. Fabula, "Linearized Theory of Vented Hydrofoils," NAVWEPS Report 7637, NOTS TP 2650, March 7, 1961.

7 M. P. Tulin, "Steady Two-Dimensional Cavity Flows About Slender Bodies," David Taylor Model Basin Report 834, May 1953.

8 T. Yao-tsu Wu, "A Simple Method for Calculating the Drag in the Linear Theory of Cavity Flows," California Institute of Technology Engineering Division Report No. 85-5, August 1957.

9 T. G. Lang, "Base-Vented Hydrofoils," NAVORD Report 6606, NOTS TP 2346, October 19, 1959.

10 M. D. van Dyke, "Subsonic Edges in Thin-Wing and Slender-Body Theory," NACA TN 3345, November 1954.

11 A. Roshko, "Pressure Distribution at the Nose of a Thin Lifting Airfoil," Douglas Aircraft Company, Inc., Report No. SM 23368, November 1958.

12 Royal Aeronautical Society Data Sheets, Aerodynamics (Controls 01.01.03 and Wings 01.01.05), 10th issue, London, England, December 1958.